Tunable Graphene-based SPR Sensors

Ergun Simsek

The George Washington University, Washington, D.C. 20052, USA

ABSTRACT

Graphene's controllable optical conductivity and mechanically strong structure make it a suitable material to design tunable localized surface plasmon resonance (LSPR) sensors. In this work, we theoretically and numerically demonstrate that the resonance wavelength of an LSPR sensor can be tuned to any value within a reasonably wide range of wavelengths by changing the voltage applied to graphene layer. Theoretical results reveal a higher sensitivity with respect to regular LSPR sensors.

Keywords: Graphene, optical sensors, surface plasmons

1. INTRODUCTION

Sensing based on surface plasmon resonance (SPR) of thin metallic layers in contact with dielectrics (such as air or fluid) has been in use for more than a half century.[1,2] This relatively old concept has experienced a major twist in mid 1990's when the availability of new nanoscale fabrication devices and techniques created previously inaccessible opportunities to structure and characterize metals on the nanometer scale and hence allowed us to control SPR properties. Initial studies have shown that the mechanism behind the SPR behavior of periodically aligned metal nanoparticles was quite different than the physics behind SPR behavior of metallic layers. In order to distinguish this dramatic difference, researchers have decided to use the term "localized SPR" (LSPR) for the resonance observed with metallic nanoparticles.[3,4] LSPR mode makes the nanoparticles absorb and scatter light so intensely that single nanoparticles are easily observed by the eye using optical scattering microscopy.[3] This phenomenon enables noble-metal nanoparticles to serve as extremely intense labels for immunoassays[5,7] and cellular imaging,[6] biochemical sensors,[7] and remote sensing.[8]

While there are several design possibilities for implementing SPR as a tool for accurate biosensing, we can broadly categorize them into two groups: bio-sensors with regular SPR and bio-sensors with LSPR.[9,10] For the former, material type, incidence angle, and thicknesses are the three main parameters, which control the resonance wavelength. Since LSPR occurs when the interaction of sub-wavelength particles with incident light yield a collective oscillation of valence electrons at their maximum strength; for the latter, not only those three parameters but also the shape, dimensions, and periodicity of nanoparticles affect the resonance wavelength. In other words, working with LSPR allows for more control over the sensor's performance.

Depending on the optical properties of the target molecules under investigation, one might need to design a sensor operating at a specific wavelength range. In this direction, either numerical methods (e.g. coupled dipole approximation[11,12] or full wave solvers (e.g. Lumerical, COMSOL, etc.) can be used under the light of basic LSPR facts. For example, the distance between each nanoparticle in a given direction should not be larger than the width of the nanoparticle in that direction in order to observe a plasmonic effect. Or, if the target wavelength is lower than the LSPR wavelength of the current design, then the inter-particle spacing should be decreased. Or, small increase in SPR wavelength can be obtained by increasing the refractive index of the material surrounding metal nanoparticles.

By following these simple rules, one can design a sensor based on the LSPR in a few tens of iterations. Once numerical results meet the design criterion, the sensor can be fabricated and tested via reflection or transmission spectroscopy. If the experimental results agree with expectations, then the designed sensor can be used several times. However, we should always remember that (i) a different type of molecule even with slightly different optical response might require another design to be detected robustly, and (ii) changing environmental conditions,

Further author information: E-mail: simsek@gwu.edu, Telephone: 1 202 994 7175.

Smart Biomedical and Physiological Sensor Technology X, edited by Brian M. Cullum, Eric S. McLamore,
Proc. of SPIE Vol. 8719, 87190S · © 2013 SPIE · CCC code: 1605-7422/13/$18 · doi: 10.1117/12.2018592

e.g. increasing temperature due to continuous illumination, might cause a severe shift in SPR wavelength and hence a severe degradation in the sensitivity of the sensor.

It is well known that multiple resonance wavelengths can be achieved by using nanoparticles with different dimensions and/or having different inter-particle distances along transverse directions. For example, Crozier *et al.* use gold nano-cylinders with 140 nm and 300 nm inter-particle spacing, and hence three distinct SPR modes (wavelengths) are generated: one for TE (s-polarized) and two* for TM (p-polarized) waves, where the resonance wavelength changes by changing the incidence angle.[19] 10 nm of red shift is observed in the SPR wavelength when the incidence angle is changed from 0 to 75 degrees. However, the sensitivity of the sensor decreases as we increase the incidence angle and especially around the light line, and this degradation can be dramatic. The fundamental challenge is determining if it is possible to design a tunable localized SPR biosensor without sacrificing the sensitivity. Our preliminary studies show that such sensors can be realized using graphene as follows.

2. DESIGN

In a typical index-of-refraction sensing setup, the change in the reflected (or transmitted) light intensity due to the change in the flow channel is monitored. Using a resonant structure might increase the contrast of the reflection (or transmission) spectra and make this monitoring easier. Assume we use metal nanoparticle (MNP) arrays as a resonant structure. As shown in Fig. 1, these MNPs can be fabricated on top of a graphene coated glass slide. In order to prevent a direct contact between graphene layer and MNPs, a thin dielectric layer might be placed. A voltage source is connected to the graphene via contacts located at two opposite ends of it. When the source is off, the device acts as a standart LSPR based sensor with a resonance wavelength where the transmission (reflection) spectrum has a minimum (maximum). Turning on the DC source changes the optical properties of graphene and the induced dipole moment of each nanoparticle, and hence the surface plasmon resonance of the whole structure. If one can control the gate voltage precisely, then the resonance wavelength of the sensor should be tuned in a reasonably wide range of wavelengths.

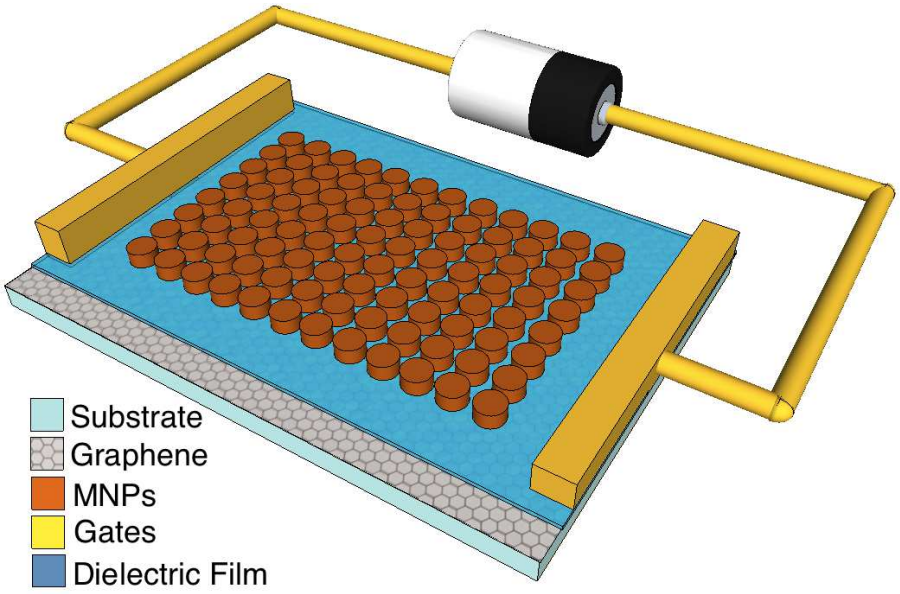

Figure 1. Metal nanoparticle (MNP) array fabricated on top of a graphene coated glass slide. A voltage source is connected to the graphene via contacts located at two opposite ends of it. For the non-contact mode, there can be a thin dielectric layer between graphene layer and MNPs.

*The non-symmetric nature of a cylinder causes two distinct resonance wavelengths for p-polarization.

3. 2D CONDUCTIVITY OF GRAPHENE BASED ON THE KUBO FORMULA

The 2D complex conductivity of graphene, which depends on the angular frequency (ω), temperature (T), and chemical potential (μ_c), can be written as $\sigma_c = \sigma_r + i\sigma_i$. According to,[20] the real and imaginary parts of the conductivity can be calculated by using

$$\sigma_r = \sigma_0 \left[\frac{18 - (\hbar\omega/t)^2}{\pi 12\sqrt{(3)}} \right] \psi_r \kappa, \tag{1}$$

where

$$\psi_r = \tanh\left(\frac{\hbar\omega + 2\mu_c}{4k_B T} \right) + \tanh\left(\frac{\hbar\omega - 2\mu_c}{4k_B T} \right), \tag{2}$$

$$\kappa = \begin{cases} \frac{1}{\sqrt{F(\hbar\omega/2t)}} \mathbf{K}\left(\frac{2\hbar\omega/t}{F(\hbar\omega/2t)} \right), & \hbar\omega < 2t \\ \frac{1}{\sqrt{2\hbar\omega/t}} \mathbf{K}\left(\frac{F(\hbar\omega/2t)}{2\hbar\omega/t} \right), & \hbar\omega \geq 2t \end{cases} \tag{3}$$

$$F(x) = (1+x)^2 - 0.25(x^2-1)^2, \tag{4}$$

$$\mathbf{K}(m) = \int_0^1 \left((1-x^2)(1-mx^2) \right)^{-1/2} dx, \tag{5}$$

and

$$\sigma_i = \frac{\sigma_0}{\pi} \left\{ \frac{4\mu_c}{\hbar\omega} \left[1 - 2\left(\frac{\mu_c}{3t} \right)^2 \right] - \left[1 - \left(\frac{\hbar\omega}{6t} \right)^2 \right] \right\} \Upsilon, \tag{6}$$

where

$$\Upsilon = \log \frac{|\hbar\omega + 2\mu_c|}{|\hbar\omega - 2\mu_c|}, \tag{7}$$

and $\sigma_0 = \pi e^2/2h$, t is hopping parameter of graphene, h and $\hbar$ are regular and reduced Planck constants, respectively, and k_B is Boltzmann constant. Fig. 2 shows real (σ_r) and imaginary (σ_i) parts of the conductivity of graphene normalized by σ_0 as a function of wavelength and chemical potential at $T = 300$ K.

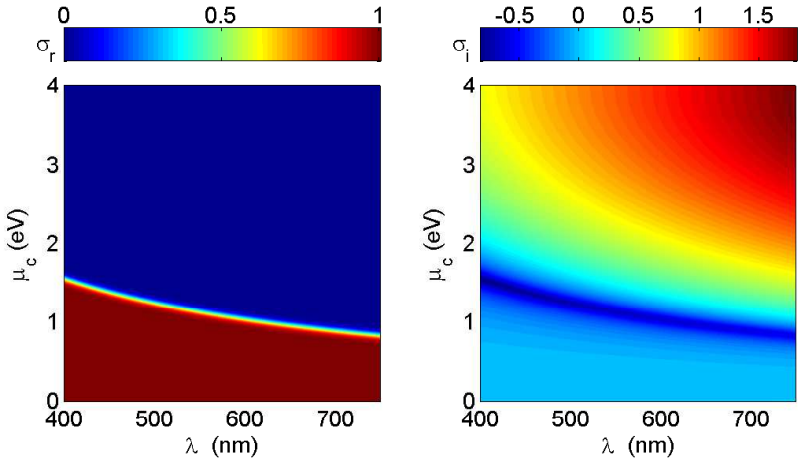

Figure 2. The real (σ_r) and imaginary (σ_i) parts of the conductivity of graphene normalized by σ_0 as a function of wavelength and chemical potential at $T = 300$ K.

4. NUMERICAL VERIFICATION OF TUNING CAPABILITY

In order to demonstrate tuning capability, the transmission spectrum is calculated for a gold cylindrical nanoparticle array fabricated on top of a graphene coated glass slide under normal incidence with ($\mu_c = 2$ eV) and without a bias voltage ($\mu_c = 0$ eV). There is a 1nm thick PMMA layer between graphene and MNP array. The thickness of graphene layer is taken as 0.34 nm. Radius and height of the cylindrical MNPs are 60 nm and 30 nm, respectively. Inter-particle spacing is 150 and 300 nm along the $\hat{x}$ and $\hat{y}$-axes, respectively. For the optical constants of gold, the experimental values are used[21] rather than Drude model to eliminate any concern regarding the selection of appropriate values for plasmon and relaxation frequencies. The dielectric constant of glass is taken as 2.13. Periodic boundary conditions are applied at the $\pm x$ and $\pm y$ boundaries. Perfectly matched layers are applied at the $\pm z$ boundaries. A grid spacing of 0.17 nm is employed.

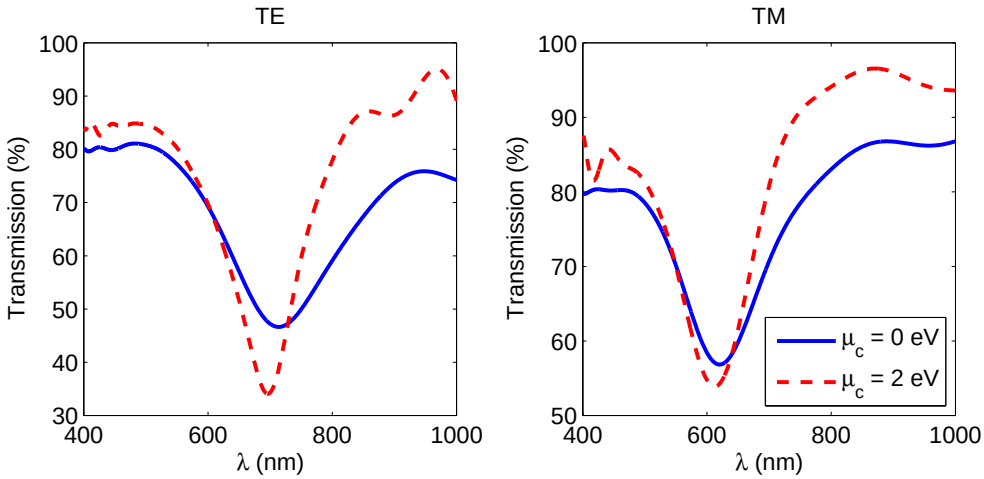

Figure 3. Transmission vs. wavelength of gold nanoparticle chain arrays for normal incidence for (left) TE polarization and (right) TM polarization.

As shown in Fig. 3, an increase of 2 eV in the chemical potential causes a 18 nm blue shift in the resonance frequency for the longitudinal mode ($\lambda_{spr} = 714$ nm and $\lambda_{spr} = 696$ nm for $\mu_c = 0$ eV and $\mu_c = 2$ eV cases, respectively). Even though the blue shift is much smaller (8 nm) for the transverse mode the transmission dip for both modes becomes narrower and sharper. As a result, unlike the broadening effect observed when the incidence angle is increased, increasing the gate voltage causes dips that are narrower and blue shifted, which facilitates monitoring.

Next, the shift of the resonance wavelength is calculated as a function of the refractive index of the top medium, where MNPs reside, to investigate the potential of the sample structure for sensing. Left and right columns of Fig. 4 show transmission through these structures for $\mu_c = 0$ eV and $\mu_c = 2$ eV cases, respectively, for TE polarization, where the refractive index of the first medium is linearly increased from 1 to 1.4. As shown in Fig. 5, the overall sensitivity of the sensor can be increased from 320 nm/RIU (refractive-index unit) to 365 nm/RIU by increasing the chemical potential from 0 to 2 eV for the longitudinal mode.

The dispersion relations are also obtained for the example design using layer medium coupled dipole approximation (LM-CDA), which is a fully-retarded theoretical model to analyze surface plasmon resonance properties of metal nanoparticle chains and arrays embedded in a multilayered medium.[12] Theoretical results, which are not shown here for the sake of brevity, are in perfect agreement with the numerical results depicted in Figures 3 and 4.

[22] presents a similar structure without a PMMA layer between metal nanoparticles and graphene in which tuning rage is slightly larger than the example presented below. This means that contact mode graphene based tunable LSPR sensor is more sensitive than its non-contact version.

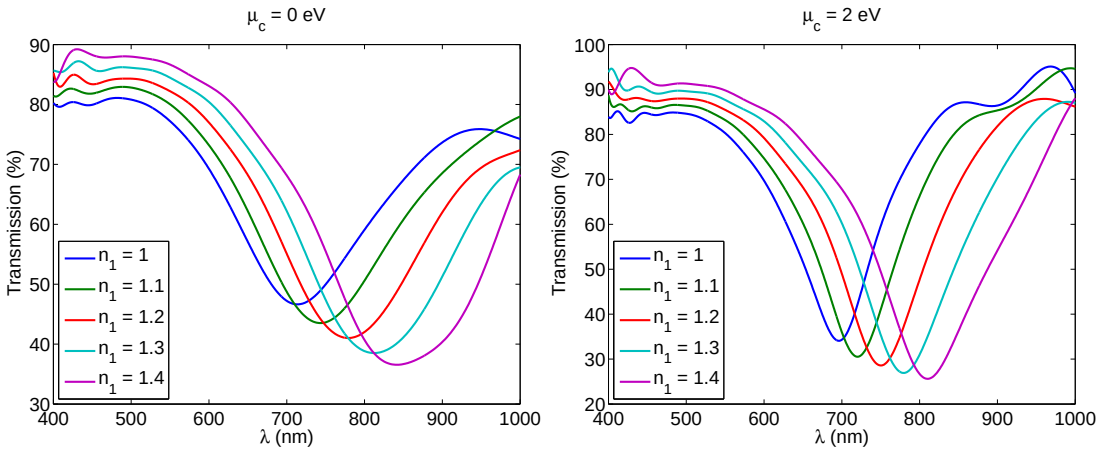

Figure 4. Transmission vs. wavelength of gold nanoparticle chain arrays for TE case normal incidence for (left) $\mu_c = 0$ eV and (right) $\mu_c = 2$ eV, where the refractive index of the first medium is linearly increased from 1 to 1.4.

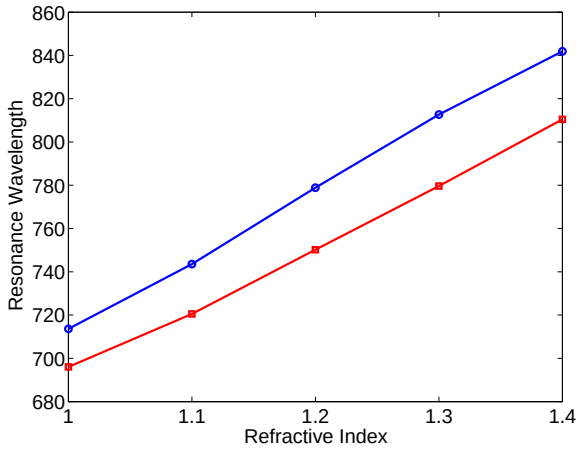

Figure 5. Longitudinal mode SPR wavelength vs. refractive index of the medium where MNPs reside. All the other parameters are same as in Fig. 3.

5. CONCLUSION

In summary, the sensitivity and tuning range of localized surface plasmon resonance sensors can be increased with graphene. Numerical and theoretical results prove that the voltage applied to the graphene layer causes a blue shift in the transmission spectra of the plasmonic sensor. In addition to a narrower transmission dip, which facilitates monitoring, the overall sensitivity of the sensor is improved as well.

REFERENCES

[1] E. Kretschmann and H. Reather, "Radiative decay of nonradiative surface plasmon excited by light," Z. Naturf. **23A**, 2135 (1968).

[2] A. Otto,"Excitation of nonradiative surface plasma waves in silver by the method of frustrated total reflection," Z. Phys. **216**, 398 (1968).

[3] X. H. N. Xu, J. Chen, R. Jeffers, S. Kyriacou, "Direct measurement of sizes and dynamics of single living membrane transporters using nano-optics," Nano Lett. **2**, 175–182 (2002).

[4] A. J. Haes, S. Zou, G. C. Schatz, R. P. Van Duyne, "Nanoscale optical biosensor: Short range distance dependence of the localized surface plasmon resonance of noble metal nanoparticles," J. Phys. Chem. B **108**, 6961–6968 (2004).

[5] S. Schultz, D. R. Smith, J. J. Mock, D. A. Schultz, "Single-target molecule detection with nonbleaching multicolor optical immunolabels," Proc. Natl Acad. Sci. USA **97**, 996–1001 (2000).
[6] A. D. McFarland and R. P. Van Duyne, "Single silver nanoparticles as real-time optical sensors with zeptomole sensitivity," Nano Lett. **3**, 1057–1062 (2003).
[7] J. M. Nam, C. S. Thaxton, C. A. Mirkin, "Nanoparticle-based bio-bar codes for the ultrasensitive detection of proteins," Science **301**, 1884–1886 (2003).
[8] R. E. Thompson, D. R. Larson, W. W. Webb, "Precise nanometer localization analysis for individual fluorescent probes," Biophys. J. **82**, 2775–2783 (2002).
[9] M. L. Brongersma and P. G. Kik. Surface Plasmon Nanophotonics. Springer (2007).
[10] R. M. Schasfoort and A. J. Tudos. Handbook of surface plasmon resonance. RSC Publishing (2008).
[11] E. Simsek, "On the Surface Plasmon Resonance Modes of Nanoparticle Chains and Arrays," Plasmonics, vol. 4, no. 3, pp. 223–230, Sept. 2009.
[12] E. Simsek, "Full Analytical Model for Obtaining Surface Plasmon Resonance Modes of Metal Nanoparticle Structures Embedded in Layered Media," Opt. Express, vol. 18, no. 2, pp. 1722–1733, Jan. 2010.
[13] K. S. Novoselov, A. K. Geim, S. V. Morozov, D. Jiang, M. I. Katsnelson, I. V. Grigorieva, S. V. Dubonos, and A. A. Firsov, "Two-dimensional gas of massless Dirac fermions in graphene," Nature, vol. 438, pp. 197-200, Sept. 2005.
[14] A. K. Geim, K. S. Novoselov, "The rise of graphene," Nature Materials, vol. 6, no. 3, pp. 183-191, Mar. 2007.
[15] J. Homola, "Present and future of surface plasmon resonance biosensors," Analytical and Bioanalytical Chemistry, vol. 377, no. 3, pp. 528-539, Oct. 2003.
[16] H. K. Hunt and A.M. Armani, "Label-free biological and chemical sensors," Nanoscale, vol. 2, no. 9, pp. 1544–59, Jun. 2010.
[17] X. Fan, I. M. White, S. I. Shopova, H. Zhu, J. D. Suter, Y. Sun, "Sensitive optical biosensors for unlabeled targets: A review," Analytical Chimica Acta, vol. 620, no. 1-2, pp. 8-26, July 2008.
[18] X. Fan and I.M. White, "Optofluidic microsystems for chemical and biological analysis," Nat Photon., vol. 5, no. 10, pp. 591–597, Sept. 2011.
[19] K. B. Crozier, E. Togan, E. Simsek, and T. Yang, "Experimental Measurement of the Dispersion Relations of the Surface Plasmon Modes of Metal Nanoparticle Chains," Opt. Express, vol. 15, pp. 17482–17493, Dec. 2007.
[20] T. Stauber, N. M. R. Peres, and A. K. Geim, "Optical conductivity of graphene in the visible region of the spectrum," Phys. Rev. B, vol. 78, pp. 085432-8, Aug. 2008.
[21] A. D. Rakic, A. B. Djurišic, J. M. Elazar, and M. L. Majewski, "Optical properties of metallic films for vertical-cavity optoelectronic devices," Appl. Opt., vol. 37, pp. 5271–5283, Aug. 1998.
[22] E. Simsek, "Improving Tuning Range and Sensitivity of Localized SPR Sensors with Graphene," to appear on IEEE Photonics Technology Letters, 2013. doi: 10.1109/LPT.2013.2253316.